Inorganic Chemistry

Article

pubs.acs.org/IC

Novel One-, Two-, and Three-Dimensional Selenidostannates Templated by Iron(II) Complex Cation

Chunying Tang, Fang Wang, Jialin Lu, Dingxian Jia,* Wenqing Jiang, and Yong Zhang

College of Chemistry, Chemical Engineering and Materials Science, Soochow University, Suzhou 215123, People's Republic of China

Supporting Information

ABSTRACT: The novel iron selenidostannates $[Fe(bipy)_3]Sn_4Se_9\cdot 2H_2O$ (**1**) and $[Fe(bipy)_3]_2[Sn_3Se_7]_2\cdot bipy\cdot 2H_2O$ (**2**) (bipy = bipyridine) were prepared by the reactions of Sn, Se, $FeCl_2\cdot 4H_2O$, bipy, and dien with/without KSCN under hydrothermal conditions (dien = diethylenetriamine). In **1**, four $SnSe_5$ units condense via edge sharing to form the novel 3-D framework selenidostannate $^3_\infty[Sn_4Se_9^{2-}]$ containing an interpenetrating channel system. The $[Fe(bipy)_3]^{2+}$ cations are accommodated in the different channels according to the conformation of the $[Fe(bipy)_3]^{2+}$ cation. In **2**, three $SnSe_5$ units share edges to form a 2-D $^2_\infty[Sn_3Se_7^{2-}]$ layered anion, while two $SnSe_5$ units and one $SnSe_4$ unit are connected via edge sharing, forming a 1-D $^1_\infty[Sn_3Se_7^{2-}]$ chainlike anion. The $^1_\infty[Sn_3Se_7^{2-}]$, $[Fe(bipy)_3]^{2+}$, bipy, and H_2O species are embedded between the $^2_\infty[Sn_3Se_7^{2-}]$ layers. **2** is the first example of a selenidostannate constructed by both $^2_\infty[Sn_3Se_7^{2-}]$and $^1_\infty[Sn_3Se_7^{2-}]$ anions. The coexistence of 1-D $^1_\infty[Sn_3Se_7^{2-}]$ and 2-D $^2_\infty[Sn_3Se_7^{2-}]$ anions in **2** might support the possible reaction mechanism that the $^2_\infty[Sn_3Se_7^{2-}]$ anions are formed by condensation of the $^1_\infty[Sn_3Se_7^{2-}]$ chains. **1** and **2** exhibit band gaps at 1.43 and 2.01 eV, respectively.

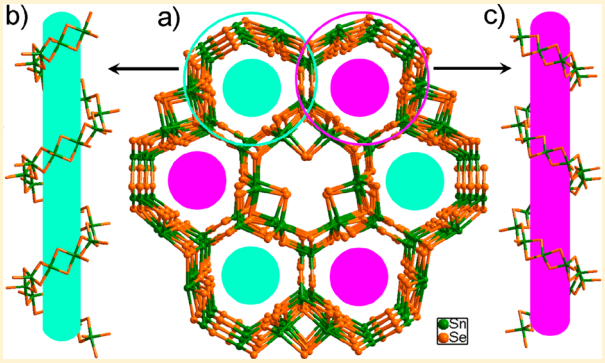

INTRODUCTION

Research on chalcogenidometalate compounds constructed by the composition of M/Ch (M = group 14 and 15 element; Ch = S, Se, Te) continues to be motivated both by their rich structural diversity based on the condensation of MCh_4 or MCh_5 primary building units via corner, edge or face sharing and by their potential applications as optical and electrical materials.[1,2] Since Bedard et al. hydrothermally prepared microporous tin and germanium sulfides in aqueous amine solution in the late 1980s,[3] the templating synthesis under mild hydro- or solvothermal conditions has been developed to be a versatile approach to the preparation of chalcogenidometalates.[4] In the case of chalcogenidostannates, much effort in templating synthesis has led to a number of binary $[Sn_xCh_y]^{n-}$ anions with different dimensional structures ranging from oligomeric anions[5] to one-dimensional (1-D) chains[5a,6] to two-dimensional (2-D) layers,[5b,c,6,7] using a variety of organic cations as structure-directing agents. The introduction of a transition metal (TM) into the binary Sn/Ch system has led to the formation of ternary $[TM_xSn_yCh_z]^{m-}$ anionic clusters or extended frameworks[8] or chalcogenidostannates combined with TM organic complexes.[9] The third types of tin chalcogenides are the lanthanide(Ln)-containing chalcogenidostannates with an organic Ln complex acting as the countercations.[10] The additions of TM and Ln increase the structural diversity of the chalcogenidostannates. A number of ternary $[TM_xSn_yCh_z]^{m-}$ anions with complicated three-dimensional (3-D) open frameworks have been obtained, giving $[Zn_4Sn_3S_{13}^{5-}]_n$, $[Zn_4Sn_3Se_{16}^{12-}]_n$,[11] $\{Sn[Zn_4Sn_4S_{17}]^{6-}\}_n$,[12] and $\{[Hg_4(\mu_4\text{-Ch})(SnCh_4)_3]^{6-}\}_n$ (Ch = Se, Te),[13] for example. However, the 3-D binary $[Sn_xCh_y]^{n-}$ anion is only observed in $[BMIm]_4Sn_9Se_{20}$ (BMIm = 1-butyl-3-methylimidazolium),[14] which was prepared by ionothermal methods.

On the other hand, the compositions and structures of chalcogenidometalates are influenced by hydrothermal or solvothermal reaction conditions. The templating synthesis is sensitive to the nature and size of structure-directing agents and a variety of reaction conditions, including reaction temperature, solvent, and the additional mineralizer.[2i,j,6] In the course of our study on the hydrothermal syntheses of chalcogenides in the presence of TM complexes,[15] we prepared iron selenidostannates $[Fe(bipy)_3]Sn_4Se_9\cdot 2H_2O$ (**1**) and $[Fe(bipy)_3]_2[Sn_3Se_7]_2\cdot bipy\cdot 2H_2O$ (**2**) under hydrothermal conditions. **1** contains a novel 3-D open-framework selenidostannate constructed by $SnSe_5$ units. **2** is the first example of a selenidostannate composed of both a $^1_\infty[Sn_3Se_7^{2-}]$ chain and $^2_\infty[Sn_3Se_7^{2-}]$layer, although compounds containing single $^1_\infty[Sn_3Se_7^{2-}]$ or $^2_\infty[Sn_3Se_7^{2-}]$ anions have been prepared for decades.

EXPERIMENTAL SECTION

Materials and Methods. All starting chemicals were analytical grade and were used as received. Elemental analyses were conducted using an EA1110-CHNS-O elemental analyzer. Fourier infrared (FT-

Received: June 12, 2014
Published: August 13, 2014

   dx.doi.org/10.1021/ic501381v | Inorg. Chem. 2014, 53, 9267−9273

IR) spectra were recorded on a Nicolet Magna-IR 550 spectrometer using dry KBr disks over the 4000−400 cm^{-1} range. Powder X-ray diffraction (PXRD) patterns were collected on a D/MAX-3C diffractometer using graphite-monochromatized Cu Kα radiation (λ = 1.5406 Å). Room-temperature optical diffuse reflectance spectra of powder samples were obtained using a Shimadzu UV-3150 spectrometer. Absorption (α/S) data were calculated from reflectance using the Kubelka−Munk function $\alpha/S = (1 - R)^2/2R$.[16] Thermal TG and DSC analyses were conducted on a SDT 2960 microanalyzer, and the samples were heated at a rate of 5 °C min^{-1} under a 100 mL min^{-1} nitrogen stream.

Synthesis of $[Fe(bipy)_3]Sn_4Se_9·2H_2O$ (1). $FeCl_2·4H_2O$ (50 mg, 0.25 mmol), Sn (59 mg, 0.5 mmol), Se (118 mg, 1.5 mmol), bipy (117 mg, 0.75 mmol), KSCN (49 mg, 0.5 mmol), and dien (0.2 mL) were dispersed in 3.0 mL of H_2O by stirring, and the dispersion was loaded into a polytetrafluoroethylene (PTFE)-lined stainless steel autoclave with an inner volume of 10 mL. The sealed autoclave was heated to 145 °C for 6 days and then was cooled to ambient temperature. Black blocklike crystals of **1** were filtered off, washed with ethanol, and dried in air. Yield: 0.177 g (81% based on Sn). Anal. Found: C, 20.48; H, 1.58; N, 4.72. Calcd for $C_{30}H_{28}N_6O_2FeSn_4Se_9$ (1745.83): C, 20.64; H, 1.62; N, 4.81. IR data (KBr, cm^{-1}): 3449 (s), 3065 (w), 1639 (w), 1597 (s), 1462 (s), 1438 (s), 1418 (m), 1310 (w), 1160 (w), 1019 (w), 882 (w), 758 (s), 729 (s), 664 (m), 531 (m), 472 (m), 418 (w).

Synthesis of $[Fe(bipy)_3]_2[Sn_3Se_7]_2·bipy·2H_2O$ (2). $FeCl_2·4H_2O$ (50 mg, 0.25 mmol), Sn (59 mg, 0.5 mmol), Se (118 mg, 1.5 mmol), bipy (117 mg, 0.75 mmol), and dien (0.2 mL) were dispersed in 3.0 mL of H_2O by stirring, and the dispersion was loaded into a PTFE-lined stainless steel autoclave with an inner volume of 10 mL. The sealed autoclave was heated to 145 °C for 6 days and then was cooled to ambient temperature. Dark red blocklike crystals of **2** were filtered off, washed with ethanol, and dried in air. Yield: 0.222 g (87% based on Sn). The reaction with Fe and $SnCl_4·5H_2O$ (or $SnCl_2·2H_2O$) instead of $FeCl_2·4H_2O$ and Sn produced the same compound of **2**. Anal. Found: C, 27.33; H, 1.85; N 6.25. Calcd for $C_{70}H_{60}N_{14}O_2Fe_2Sn_6Se_{14}$ (3058.60): C, 27.49; H, 1.98; N, 6.41. IR data (KBr, cm^{-1}): 3444 (w), 3052 (w), 3010 (w), 1592 (s), 1473 (s), 1438 (s), 1306 (m), 1250 (w), 1165 (m), 1053 (m), 1010 (s), 895 (w), 771 (s), 738 (s), 651 (s), 624 (w), 415 (m).

Single-Crystal X-ray Diffraction. Data were collected on a Rigaku Saturn CCD diffractometer at 293(2) K using graphite-monochromated Mo Kα radiation (λ = 0.71073 Å) to a maximum 2θ value of 50.70°. The intensity data sets were collected with a ω-scan method and reduced with the CrystalClear program.[17] An empirical absorption correction was applied for compounds **1** and **2** using the multiscan method. The structures were solved by direct methods using the program SHELXS-97[18a] and were refined using a full-matrix least-squares refinement on F^2 using SHELXL-97.[18b] All of the non-hydrogen atoms were refined anisotropically. The hydrogen atoms were added geometrically and refined as a riding model. Hydrogen atoms of water molecules were not added. Technical details of data acquisition and selected refinement results are summarized in Table 1.

Table 1. Crystal Data and Summary of X-ray Data Collection

	1	2
formula	$C_{30}H_{28}N_6O_2FeSn_4Se_9$	$C_{70}H_{60}N_{14}O_2Fe_2Sn_6Se_{14}$
M_r	1745.83	3058.60
cryst syst	hexagonal	monoclinic
space group	$R3c$ (No. 161)	$P2_1/c$ (No. 14)
a, Å	26.902(4)	27.055(5)
b, Å	26.902(4)	13.391(3)
c, Å	30.673(6)	24.756(5)
β, deg	90	103.88(3)
V, Å^3	19224(5)	8707(3)
Z	18	4
T, K	293(2)	293(2)
D_{calcd} (g cm^{-3})	2.715	2.333
$F(000)$	14364	5688
2θ(max), deg	50.70	50.70
total no. of rflns collected	60728	35134
no. of unique rflns	7794	15799
R_{int}	0.0702	0.0672
no. of params	505	963
R1 ($I > 2\sigma(I)$)	0.0406	0.0456
wR2 (all data)	0.0991	0.0980
GOF on F^2	1.111	1.124

RESULTS AND DISCUSSION

Syntheses. The reaction of Sn, Se, $FeCl_2·4H_2O$, KSCN, bipy, and dien in aqueous solution at 145 °C for 6 days produced black crystals of $[Fe(bipy)_3]Sn_4Se_9·2H_2O$ (**1**). The reaction without KSCN under the same conditions afforded dark red blocklike crystals of $[Fe(bipy)_3]_2[Sn_3Se_7]_2·bipy·2H_2O$ (**2**). The addition of 0.5−1.0 mmol of KSCN produced the same compound of **1**. However, the role of KSCN is not yet clear. Compounds **1** and **2** can be obtained in the temperature range 145−170 °C. In all of the syntheses, the amine dien is needed. SnO_2 or $SnCl_4$ can be used instead of elemental Sn as the source for Sn^{4+} cations with yields of 52−68%. The bulk phase purity of compounds **1** and **2** was measured by a powder XRD study. The experimental PXRD patterns are similar to the simulated PXRD patterns on the basis of the single-crystal X-ray diffraction data, respectively (Figures S1 and S2 in the Supporting Information). In the IR spectra of **1** and **2** (Figures S3 and S4 in the Supporting Information), absorption bands in the frequency range 3010−3065 cm^{-1} are due to the C−H vibrations of the aromatic ring hydrogen atoms of bipy ligands. The broad absorption bands in the range of 3450 and 3445 cm^{-1} are assigned to the O−H modes of H_2O. The absorption bands in the range 1592−1438 cm^{-1} correspond to ring vibrations of the bipy ligand.

Crystal Structures. Compound **1** crystallizes in the hexagonal space group $R3c$ with 18 formula units in the unit cell. It consists of a $[Fe(bipy)_3]^{2+}$ complex cation, a 3-D polymeric $^3_\infty[Sn_4Se_9^{2-}]$ anion, and two lattice water molecules. The Fe^{2+} ion is coordinated by three bipy ligands, forming a slightly distorted octahedral $[Fe(bipy)_3]^{2+}$ complex cation, as demonstrated by the axial and equatorial angles (Table 2). The Fe−N bond lengths are similar to those observed in the reported Fe(II) complexes with a bipy ligand.[19] The polymeric $^3_\infty[Sn_4Se_9^{2-}]$ anion contains four crystallographically independent Sn^{4+} ions and nine Se^{2-} ions. Each of the Sn^{4+} ions is coordinated to five Se^{2-} anions at distances in the range 2.483(3)−2.828(2) Å, forming the $SnSe_5$ primary building unit (PBU). All $SnSe_5$ PBUs have a distorted-trigonal-bipyramidal symmetry geometry (Table 2). The Sn−Se bond lengths and Se−Sn−Se angles are in accordance with those observed in the selenidostannates constructed by the $SnSe_5$ PBU.[7]

Three $SnSe_5$ PBUs (containing Sn1, Sn2, and Sn3) share edges to form a Sn_3Se_{10} secondary building unit (SBU), in which three Sn atoms are capped by a μ_3-Se atom and are joined by three μ_2-Se atoms to form a Sn_3Se_4 "semi-cube" (Figure 1a). Three Sn_3Se_{10} SBUs are alternatively connected by three $Sn(4)Se_5$ PBUs into a circular $Sn_{12}Se_{33}$ unit via edge sharing, which contains a 12-membered Sn_6Se_6 ring (Figure 1a). The Se^{2-} anions adopt μ_3-Se (Se1, Se3) and μ-Se (Se2, Se4−Se9) bridging coordination modes to the Sn^{4+} ions in the asymmetric $[Sn_4Se_9]^{2-}$ unit of compound **2**. As shown in Figure 1b, each $Sn_{12}Se_{33}$ unit is further connected with six other

dx.doi.org/10.1021/ic501381v | Inorg. Chem. 2014, 53, 9267−9273

Table 2. Selected Bond Lengths (Å) and Angles (deg) for 1 and 2

	1	2
Sn−Se[a]	2.483(3)−2.828(2)	2.512(2)−2.8273(19)
Sn−Se[b]		2.408(2)−2.599(2)
Fe−N	1.954(16)−1.999(16)	1.931(11)−1.995(12)
Se−Sn−$Se_{equatorial}$[a]	82.92(9)−124.98(9)−	86.22(6)−131.18(6)
Se−Sn−Se_{axial}[a]	169.33(8)−177.34(8)	174.37(5)−178.84(6)
Se−Sn−Se[b]		92.46(6)−128.09(7)
Sn−Se−Sn	84.92(9)−119.60(7)	81.0(5)−94.56(6)
N−Fe−N_{axial}	173.7(6)−176.3(6)	172.7(5)−176.4(5)
N−Fe−$N_{equatorial}$	81.4(7)−95.5(7)	81.2(5)−96.1(5)

[a]Bond lengths and angles of the $SnSe_5$ unit. [b]Bond lengths and angles of the $SnSe_4$ unit.

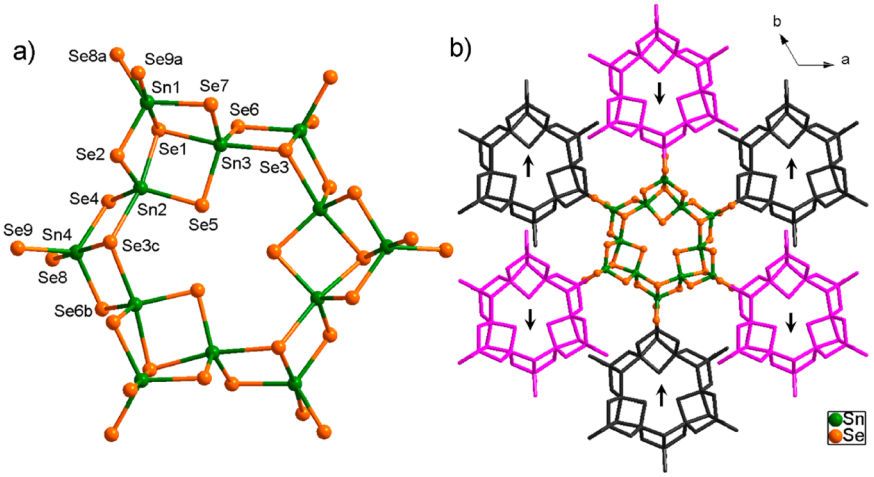

Figure 1. (a) Structure of the $Sn_{12}Se_{33}$ unit in **1**, showing the asymmetric Sn_4Se_9 unit with the labeling scheme. (b) Linkage between the $Sn_{12}Se_{33}$ units in **1**, showing the $Sn_{12}Se_{33}$ units propagating up (in black) and down (in purple) the central unit viewed along the [001] axis.

$Sn_{12}Se_{33}$ units via edge sharing at Se8 and Se9 atoms. Three $Sn_{12}Se_{33}$ units (Figure 1b, shown in black) are located up the plane defined by the central $Sn_{12}Se_{33}$ unit, while three $Sn_{12}Se_{33}$ units (Figure 1b, shown in purple) are located down the plane. The planes of all the $Sn_{12}Se_{33}$ units are perpendicular to the [001] axis (Figure 1b). As a result, the $Sn_{12}Se_{33}$ units propagate to form the polymeric $^3_\infty[Sn_4Se_9^{2-}]$anion with a 3-D structure. The propagation of $Sn_{12}Se_{33}$ units generates a channel system, formed by connected helical chains of the linked $SnSe_5$ PBUs as channel walls. The channels running along the [001] axis have a cross-sectional diameter of 8.3 Å, and each $Sn_{12}Se_{33}$ unit is surrounded by six such channels (Figures 2a and 3a). The channels are formed by helical chainlike $SnSe_5$ linkages along the [001] axis. The left-handed (Figure 2b) and right-handed (Figure 2c) helices occur alternately around the $Sn_{12}Se_{33}$ units. $[Fe(bipy)_3]^{2+}$ ions and H_2O molecules are located in the channels (Figures S5 and S6 in the Supporting Information). The $[Fe(bipy)_3]^{2+}$ ions in the channels formed by right-handed helices are in the Δ conformation, while the $[Fe(2,2'\text{-bipy})_3]^{2+}$ ions in the left-handed channels are in the Λ conformation (Figure S5). Other channels run along the [100], [010], and [101] directions and have cross-sectional dimensions of 14.9 × 5.8 (in the [100] and [010] directions) and 17.9 × 9.6 $Å^2$, respectively (Figure 3b,c).

The high tendency for copolymerization of the $SnSe_4$ and $SnSe_5$ PBUs via corner, edge, or face sharing had led to a series of binary selenidostannates with different compositions and structures ranging from discrete anions[5] to infinite chains[5a,6] to two-dimensional sheets,[5b,c,6,7,9e,20,21] depending on the structure-directing agents or countercations used in the syntheses. However, selenidostannates with three-dimensional constructs are very rare. The compound $[BMIm]_4Sn_9Se_{20}$,[14] which was prepared using an organic cation as counterion under ionothermal conditions, is the only example of a selenidostannate containing a 3-D framework. The anion is composed of both $SnSe_4$ and $SnSe_5$ PBUs via edge and face sharing. The 3-D selenidostannate constructed by a sole $SnSe_5$ trigonal bipyramid has not been observed before. **1** represents the first 3-D framework selenidostannate constructed by a $SnSe_5$ trigonal bipyramid and containing TM complex countercations. Thus,

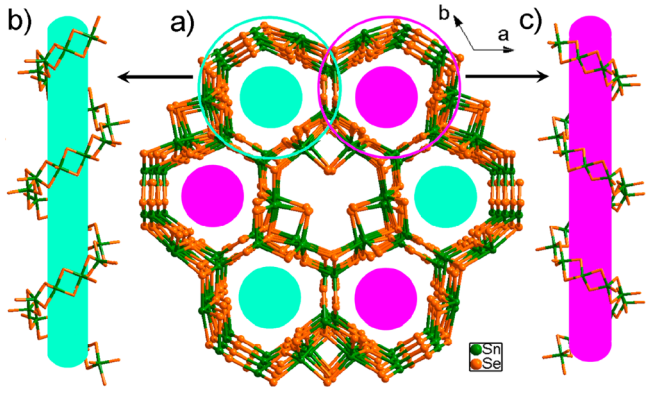

Figure 2. (a) Crystal packing diagram of **1** viewed down the [001] axis. $[Fe(bipy)_3]^{2+}$ ions and H_2O molecules are omitted for clarity. (b) Channel formed by left-handed helical Sn−Se linkages. (c) Channel formed by right-handed helical Sn−Se linkages.

dx.doi.org/10.1021/ic501381v | Inorg. Chem. 2014, 53, 9267−9273

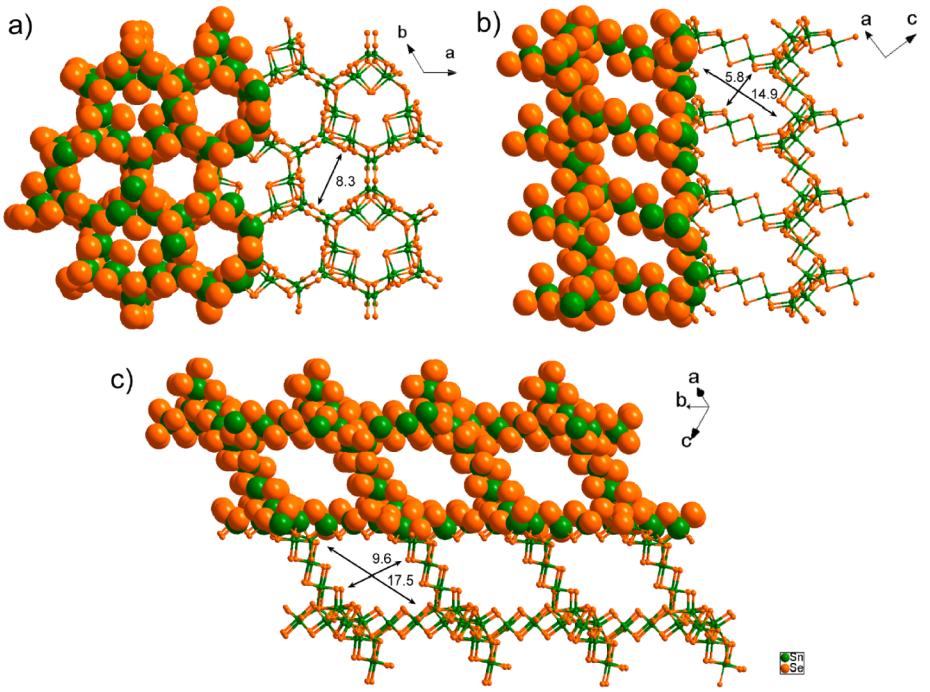

Figure 3. Extending structures of the $^{3}_{\infty}[Sn_4Se_9^{2-}]$anion in **1**, showing the channels running along the [001] (a), [010] (b), and [101] (c) directions. Values are given in angstroms. The $[Fe(bipy)_3]^{2+}$ ions and H_2O molecules are omitted for clarity.

the formation of a 3-D selenidostannate anion based on the $SnSe_5$ trigonal bipyramids in **1** is unique. It is worth noting that the compound $A_2Sn_4Se_9{\cdot}H_2O$ (A = Rb, Cs) exhibits a structure completely different from that of **1**,[20] even though it has the same anionic composition as that of **1**. The compound $A_2Sn_4Se_9{\cdot}H_2O$ consists of a $^{2}_{\infty}[Sn_4Se_9^{2-}]$ layered anion that is constructed by the tetrahedral $SnSe_4$ PBUs.

Compound **2** crystallizes in the monoclinic space group $P2_1/c$ with 4 formula units in the unit cell. It consists of two $[Fe(bipy)_3]^{2+}$ complex cations, a two-dimensional $^{2}_{\infty}[Sn_3Se_7^{2-}]$ anion, a one-dimensional $^{1}_{\infty}[Sn_3Se_7^{2-}]$ anion, a free bipy molecule, and two lattice water molecules. Both $Fe(1)^{2+}$ and $Fe(2)^{2+}$ are coordinated by three bipy ligands, forming octahedral $[Fe(bipy)_3]^{2+}$ complexes with a structure similar to that of the Fe(II) complex cation in **1** (Tables S1 and S2 in the Supporting Information). Compound **2** contains 6 crystallographically independent Sn^{4+} ions and 14 Se^{2-} ions. Except for the $Sn(4)^{4+}$ ion, which is in a tetrahedral coordination sphere, the other five Sn^{4+} ions are coordinated to five Se^{2-} anions, forming $SnSe_5$ trigonal-bipyramidal PBUs. The Sn−Se bond lengths of the $SnSe_5$ units are in the range 2.512(2)−2.8273(19) Å (Table 2) and are in accordance with those observed in **1**, except for the Sn(6)−Se(9) bond, which has a longer length of 3.136(2) Å (Table S2). In **2**, the Sn−Se bond lengths of the $SnSe_4$ (Sn−Se = 2.408(2)−2.599(2) Å) unit are in the lower range of the equatorial Sn−Se bond lengths of $SnSe_5$ (Sn−Se = 2.5125(18)−2.631(2) Å) but are obviously shorter than those of the axial Sn−Se bond lengths of $SnSe_5$ (Sn−Se = 2.6751(19)−2.8273(19) Å) (Table 2 and Table S2 in the Supporting Information).

Three $SnSe_5$ PBUs (containing Sn1, Sn2, and Sn3) share edges to form a Sn_3Se_{10} SBU containing a Sn_3Se_4 "semicube". Each Sn_3Se_{10} SBU is connected to three other Sn_3Se_{10} SBUs via edge sharing (at Se6 and Se7) to form the layered $^{2}_{\infty}[Sn_3Se_7^{2-}]$ anion (Figure 4a). As a result, the interconnection of the Sn_3Se_{10} SBUs generates a honeycomb structure containing 24-membered $Sn_{12}Se_{12}$ rings in the $^{2}_{\infty}[Sn_3Se_7^{2-}]$ layers (Figure 5b). The $Sn_{12}Se_{12}$ rings are formed by six Sn_3Se_4 semicubes interlinked by 12 μ_2-Se atoms. Two $SnSe_5$ PBUs (containing Sn5 and Sn6) and one $SnSe_4$ PBU are joined end to end via

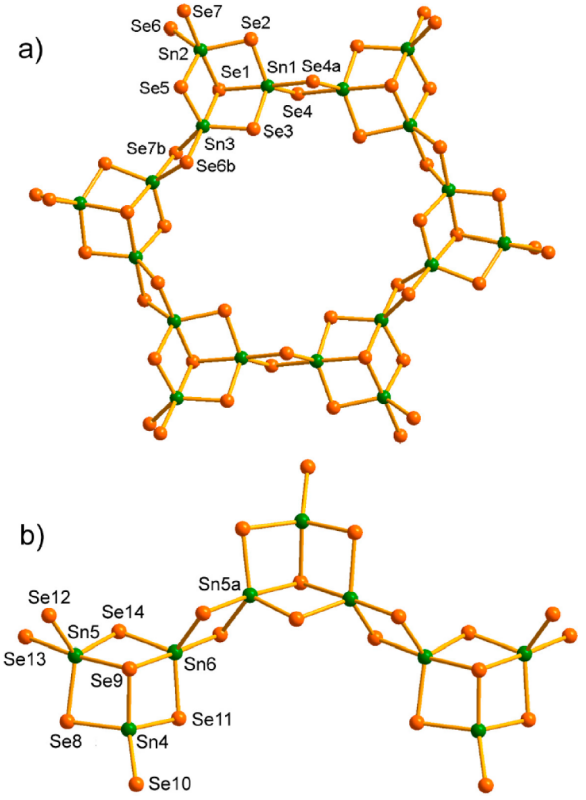

Figure 4. Structures of (a) the Sn_3Se_{10} subunit of the $^{2}_{\infty}[Sn_3Se_7^{2-}]$layer and (b) the Sn_3Se_9 subunit of the $^{1}_{\infty}[Sn_3Se_7^{2-}]$ chain in **2**, showing the asymmetric Sn_3Se_7 units with the labeling scheme.

dx.doi.org/10.1021/ic501381v | Inorg. Chem. 2014, 53, 9267−9273

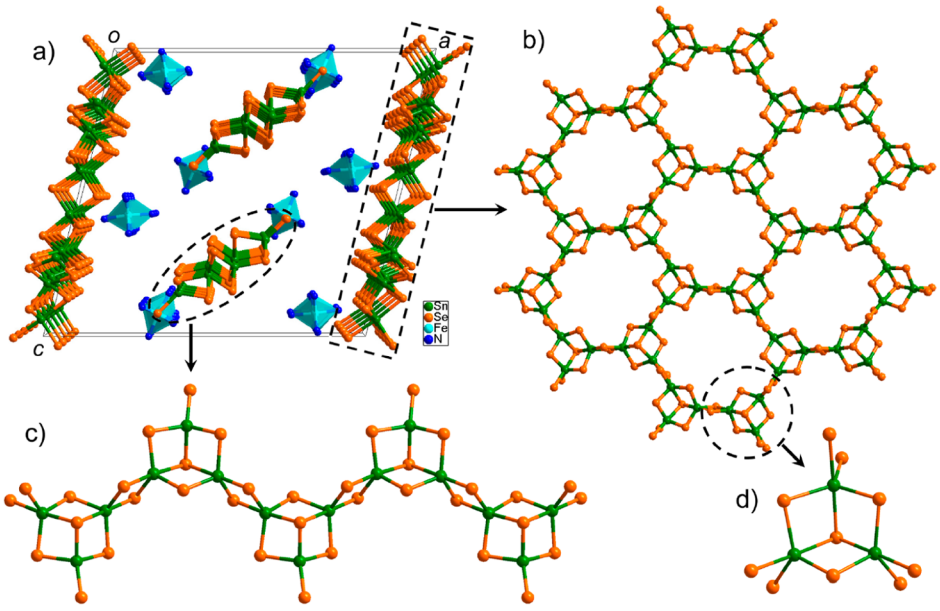

Figure 5. (a) Packing diagram of **2** viewed down the [010] axis. C and H atoms of $[Fe(bipy)_3]^{2+}$ and lattice bipy and H_2O molecules are omitted for clarity. Cyan octahedron: FeN_6. (b) Structure of the $^2_\infty[Sn_3Se_7^{2-}]$ layer in **2**. (c) Structure of the $^1_\infty[Sn_3Se_7^{2-}]$ chain in **2**. (d) Structure of the Sn_3Se_{10} SBU in $^2_\infty[Sn_3Se_7^{2-}]$.

edge sharing to form a Sn_3Se_9 SBU, which also contains a Sn_3Se_4 semicube. The Sn_3Se_9 SBUs are connected via edge sharing at Se12 and Se13 into a one-dimensional $^1_\infty[Sn_3Se_7^{2-}]$ chain (Figure 4b). The $^1_\infty[Sn_3Se_7^{2-}]$ chains run parallel to the [010] axis (Figure 5a). The $^1_\infty[Sn_3Se_7^{2-}]$ chains, $[Fe(bipy)_3]^{2+}$ cations, H_2O, and free bipy molecules are embedded between the $^2_\infty[Sn_3Se_7^{2-}]$ layers, which are perpendicular to the [100] axis (Figure 5a). The $[Fe(2)(bipy)_3]^{2+}$ cations are located at both sides of the $^1_\infty[Sn_3Se_7^{2-}]$ chain (Figure S7 in the Supporting Information), while the $[Fe(1)(bipy)_3]^{2+}$ cations suspend up and down the honeycomb holes of the $^2_\infty[Sn_3Se_7^{2-}]$ layer with a pyridine ring inserting into the hole (Figure S8 in the Supporting Information).

Two different modifications are observed for the $^2_\infty[Sn_3Se_7^{2-}]$ layered anions. The $^2_\infty[Sn_3Se_7^{2-}]$ layer in **2** contains a 24-membered $Sn_{12}Se_{12}$ "rectangular ring" with cross sectional dimensions of 13.478 × 10.184 Å (Figure S9 in the Supporting Information). Several chalcogenidostannates containing the $^2_\infty[Sn_3Se_7^{2-}]$ layered anions have been prepared to date using alkali-metal cations,[7a] organic cations,[5b,c,7b−f] and TM complex cations[9e] as the counterions. All of the 2-D anions in these reported chalcogenidostannates have the structures and connections similar to those of the $^2_\infty[Sn_3Se_7^{2-}]$ anion in **2**, but they possess the "round ring" $Sn_{12}Se_{12}$. The $^2_\infty[Sn_3Se_7^{2-}]$ anion in $[Fe(phen)_3]Sn_3Se_7{\cdot}1.25H_2O$,[9e] for example, contains 24-membered round rings with a diameter of 11.305 Å (Figure S9). In the$^2_\infty[Sn_3Se_7^{2-}]$ anion, each Sn_3Se_4 semicube is connected with three other Sn_3Se_4 units via three double μ-Se bridges. The three dihedral angles around the three double μ-Se bridges in the $^2_\infty[Sn_3Se_7^{2-}]$ anion of $[Fe(phen)_3]Sn_3Se_7{\cdot}1.25H_2O$ are identical and are equal to −1.82°. However, the corresponding angles of the $^2_\infty[Sn_3Se_7^{2-}]$ anion in **2** are 0.0, 9.52(3), and 10.10(3)° (Table S2 in the Supporting Information), which causes formation of the rectangular $Sn_{12}Se_{12}$ ring.

The striking feature of **2** is the coexistence of 1-D $^1_\infty[Sn_3Se_7^{2-}]$ and 2-D $^2_\infty[Sn_3Se_7^{2-}]$ anions in one compound. The $^2_\infty[Sn_3Se_7^{2-}]$ layered anions have been commonly observed as salts of a variety of cations.[5b,c,7,9e] Sheldrick proposed that the $^2_\infty[Sn_3Se_7^{2-}]$ layered anion would be formed by condensation of the single $^1_\infty[Sn_3Se_7^{2-}]$ chains via a concerted nucleophilic attack of the terminal Se atoms on the tetrahedral Sn atoms of the adjacent $^1_\infty[Sn_3Se_7^{2-}]$ chains.[4d,5a] However, the $^1_\infty[Sn_3Se_7^{2-}]$ chain has not been isolated from the synthetic solutions, except for the lone example of $(Et_4N)_2Sn_3Se_7$,[5a] which was prepared in CH_3OH solution using $(Et_4N)I$ as the structure-directing agent under solvothermal conditions. Recently, a $[Sn_3Se_7^{2-}]_\infty$ double chain has been ionothermally prepared, which is regarded as a possible "intermediate product" of the reaction pathway from a single chain to a layer.[6] The coexistence of the $^1_\infty[Sn_3Se_7^{2-}]$ and $^2_\infty[Sn_3Se_7^{2-}]$ anions in a single compound of **2** is another example to strongly support the proposed reaction mechanism from $^1_\infty[Sn_3Se_7^{2-}]$ chains to a $^2_\infty[Sn_3Se_7^{2-}]$ layer.

Optical Properties. The UV−vis reflectance spectra of the title compounds were measured on powder samples at room temperature. The absorption data from the reflectance spectra by the Kubelka−Munk function[16] demonstrate that compound **1** exhibits a steep absorption edge with a band gap (E_g) at 1.43 eV, which is smaller than that of the 3-D $[BMIm]_4[Sn_9Se_{20}]$.[14] Compound **2** shows an absorption edge with band gaps at 2.01 eV (Figure 6). The band gap is comparable to that of the Fe selenidostannates $[Fe(phen)_3]Sn_3Se_7{\cdot}1.25H_2O$ (E_g = 1.97 eV), containing a $^2_\infty[Sn_3Se_7^{2-}]$ anionic layer.[9e] The broad absorption at 4.30 eV (288.5 nm) may be attributed to the intraligand $\pi \rightarrow \pi^*$ transition occurring in bipy.

Thermal Properties. The thermal stabilities of the title compounds were investigated by TG-DSC methods under a nitrogen atmosphere in the temperature range 25−500 °C. The TGA curve shows that compound **1** decomposes in two steps with mass losses of 2.7% in the first step and 27.1% in the second step (Figure S10 in the Supporting Information). The mass losses are in agreement with complete removals of the H_2O molecules (theoretical mass loss 2.1%) and bipy (theoretical mass loss 26.8%), respectively. The decomposition process is accompanied by two endothermic signals in the DSC

dx.doi.org/10.1021/ic501381v | Inorg. Chem. 2014, 53, 9267−9273

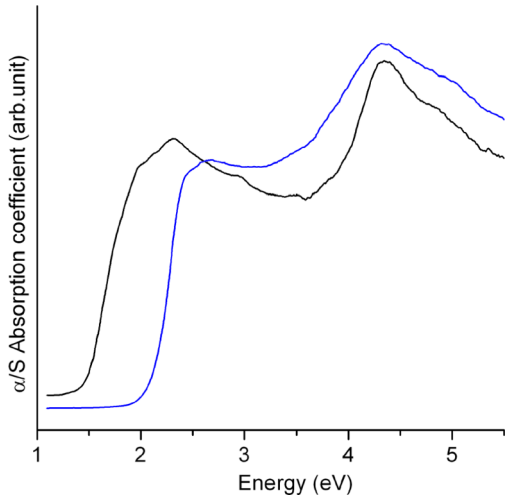

Figure 6. Solid-state optical absorption spectra of compounds **1** (black) and **2** (blue).

curve with peak temperatures at 142 and 323 °C. Compound **2** also decomposes in a two-step process. It loses two H_2O molecules and one free bipy molecule (mass loss theoretical 6.3%, observed 5.8%) between 120 and 270 °C in the first step. In the second step, it removes all bipy ligands with a total mass loss of 30.1% (theoretical mass loss 30.6%) between 275 and 375 °C.

CONCLUSION

In summary, the novel selenidostannates **1** containing a 3-D $^{3}_{\infty}[Sn_4Se_9^{2-}]$ open framework, and **2** containing mixed 2-D $^{2}_{\infty}[Sn_3Se_7^{2-}]$ and 1-D $^{1}_{\infty}[Sn_3Se_7^{2-}]$ anions were first prepared using the $[Fe(bipy)_3]^{2+}$ complex cation formed in situ as a structure-directing agent under solvothermal conditions. The synthesis of **2** confirms the existence of 1-D $^{1}_{\infty}[Sn_3Se_7^{2-}]$ and 2-D $^{2}_{\infty}[Sn_3Se_7^{2-}]$ anions in a single compound, which might support the proposed reaction pathway that the $^{2}_{\infty}[Sn_3Se_7^{2-}]$ anions would be formed by condensation of the single $^{1}_{\infty}[Sn_3Se_7^{2-}]$ chains.

ASSOCIATED CONTENT

Supporting Information

CIF files giving crystallographic data of **1** and **2**, selected bond lengths and angles for **1** and **2** (Tables S1 and S2), PXRD patterns (Figures S1 and S2), IR spectra (Figures S3 and S4), structural figures (Figures S5–S9), and TG-DSC curves (Figure S10). This material is available free of charge via the Internet at http://pubs.acs.org.

AUTHOR INFORMATION

Corresponding Author

*E-mail for D.J.: jiadingxian@suda.edu.cn.

Notes

The authors declare no competing financial interest.

ACKNOWLEDGMENTS

This work was supported by the National Natural Science Foundation of China (NSFC, No. 21171123) and the project funded by the Priority Academic Program Development (PAPD) of Jiangsu Higher Education Institutions.

REFERENCES

(1) (a) Zheng, N.; Bu, X.; Wang, B.; Feng, P. *Science* **2002**, *298*, 2366–2369. (b) Hsu, K. F.; Loo, S.; Guo, F.; Chen, W.; Dyck, J. S.; Uher, C.; Hogan, T.; Polychroniadis, E. K.; Kanatzidis, M. G. *Science* **2004**, *303*, 818–821. (c) Trikalitis, P. N.; Rangan, K. K.; Kanatzidis, M. G. *J. Am. Chem. Soc.* **2002**, *124*, 2604–2613. (d) Karkamkar, A. J.; Kanatzidis, M. G. *J. Am. Chem. Soc.* **2006**, *128*, 6002–6003. (e) Bag, S.; Trikalitis, P. N.; Chupas, P. J.; Kanatzidis, M. G. *Science* **2007**, *317*, 490–493. (f) Haddadpour, S.; Melullis, M.; Staesche, H.; Mariappan, C. R.; Roling, B.; Clérac, R.; Dehnen, S. *Inorg. Chem.* **2009**, *48*, 1689–1698. (g) Brandmayer, M. K.; Clérac, R.; Weigend, F.; Dehnen, S. *Chem.—Eur. J.* **2004**, *10*, 5147–5157. (h) Manos, M. J.; Kanatzidis, M. G. *J. Am. Chem. Soc.* **2009**, *131*, 6599–6607. (i) Manos, M. J.; Jang, J. I.; Ketterson, J. B.; Kanatzidis, M. G. *Chem. Commun.* **2008**, *8*, 972–974. (j) Chung, I.; Song, J. H.; Jang, J. I.; Freeman, A. J.; Ketterson, J. B.; Kanatzidis, M. G. *J. Am. Chem. Soc.* **2009**, *131*, 2647–2656. (k) Zhang, Q.; Chung, I.; Jang, J. I.; Ketterson, J. B.; Kanatzidis, M. G. *J. Am. Chem. Soc.* **2009**, *131*, 9896–9897. (l) Bag, S.; Kanatzidis, M. G. *J. Am. Chem. Soc.* **2010**, *132*, 14951–14959. (m) Manos, M. J.; Kanatzidis, M. G. *Inorg. Chem.* **2009**, *48*, 4658–4660.

(2) (a) Stephan, H. O.; Kanatzidis, M. G. *J. Am. Chem. Soc.* **1996**, *118*, 12226–12227. (b) Chou, J.-H.; Hanko, J. A.; Kanatzidis, M. G. *Inorg. Chem.* **1997**, *36*, 4–9. (c) Wachhold, M.; Kanatzidis, M. G. *Inorg. Chem.* **1999**, *38*, 3863–3870. (d) Wachhold, M.; Kanatzidis, M. G. *Inorg. Chem.* **2000**, *39*, 2337–2343. (e) Choi, K.-S.; Kanatzidis, M. G. *Chem. Mater.* **2000**, *39*, 5655–5662. (f) Bensch, W.; Näther, C.; Stähler, R. *Chem. Commun.* **2001**, 477–478. (g) Stähler, R.; Mosel, B. D.; Eckert, H.; Bensch, W. *Angew. Chem., Int. Ed.* **2002**, *41*, 4487–4489. (h) Vaqueiro, P.; Chippindale, A. M.; Powell, A. V. *Inorg. Chem.* **2004**, *43*, 7963–7965. (i) Stähler, R.; Bensch, W. *Z. Anorg. Allg. Chem.* **2002**, *628*, 1657–1662. (j) Schaefer, M.; Näther, C.; Lehnert, N.; Bensch, W. *Inorg. Chem.* **2004**, *43*, 2914–2921. (k) Bera, T. K.; Jang, J. I.; Song, J.-H.; Malliakas, C. D.; Freeman, A. J.; Ketterson, J. B.; Kanatzidis, M. G. *J. Am. Chem. Soc.* **2010**, *132*, 3484–3495. (l) Seidlhofer, B.; Näther, C.; Bensch, W. *CrystEngChem* **2012**, *14*, 5441–5445.

(3) Bedard, R. L.; Milson, S. T.; Vail, L. D.; Bennett, J. M.; Flanigen, E. M. *Stud. Surf. Sci. Catal. A* **1989**, *49*, 375.

(4) (a) Sheldrick, W. S.; Wachhold, M. *Coord. Chem. Rev.* **1998**, *176*, 211–322. (b) Li, J.; Chen, Z.; Wang, R. J.; Proserpio, D. M. *Coord. Chem. Rev.* **1999**, *190–192*, 707–735. (c) Dehnen, S.; Melullis, M. *Coord. Chem. Rev.* **2007**, *251*, 1259–1280. (d) Sheldrick, W. S. *J. Chem. Soc., Dalton Trans.* **2000**, 3041–3052. (e) Kromm, A.; Almsick, T. V.; Sheldrick, W. S. *Z. Naturforsch., B* **2010**, *65b*, 918–936. (f) Wachter, J. *Coord. Chem. Rev.* **2010**, *254*, 2078–2085.

(5) (a) Loose, A.; Sheldrick, W. S. *Z. Anorg. Allg. Chem.* **1999**, *625*, 233–240. (b) Fehlker, A.; Blachnik, R. *Z. Anorg. Allg. Chem.* **2001**, *627*, 1128–1134. (c) Fehlker, A.; Blachnik, R. *Z. Anorg. Allg. Chem.* **2001**, *627*, 411–418. (d) Loose, A.; Sheldrick, W. S. *Z. Anorg. Allg. Chem.* **2001**, *627*, 2051–2052. (e) Park, C.; Pell, M. A.; Ibers, J. A. *Inorg. Chem.* **1996**, *35*, 4555–4558. (f) Li, J.; Marler, B.; Kessler, H.; Soulard, M.; Kallus, S. *Inorg. Chem.* **1997**, *36*, 4697–4701. (g) Ko, Y.; Tan, K.; Nellis, D. M.; Koch, S.; Parise, J. B. *J. Solid State Chem.* **1995**, *114*, 506–511.

(6) Li, J. R.; Xiong, W. W.; Xie, Z. L.; Du, C. F.; Zou, G. D.; Huang, X. Y. *Chem. Commun.* **2013**, *49*, 181–183.

(7) (a) Sheldrick, W. S.; Braunbeck, H. G. *Z. Naturforsch., B* **1990**, *45b*, 1643–1646. (b) Parise, J. B.; Ko, Y.; Rijssenbeek, J.; Nellis, D. M.; Tan, K.; Koch, S. *Chem. Commun.* 1994, 527. (c) Jiang, T.; Lough, A.; Ozin, G. A. *Adv. Mater.* **1998**, *10*, 42–46. (d) Xu, G.-H.; Wang, C.; Guo, P. *Acta Crystallogr.* **2009**, *65C*, m171–m173. (e) Sheldrick, W. S.; Braunbeck, H. G. *Z. Anorg. Allg. Chem.* **1993**, *619*, 1300–1306. (f) Lu, S.; Ke, Y.; Li, J.; Zhou, S.; Wu, X.; Du, W. *Struct. Chem.* **2003**, *14*, 637–642.

(8) (a) Zimmermann, C.; Anson, C. E.; Weigend, F.; Clérac, R.; Dehnen, S. *Inorg. Chem.* **2005**, *44*, 5686–5695. (b) Zimmermann, C.; Melullis, M.; Dehnen, S. *Angew. Chem.* **2002**, *114*, 4444–4447. (c) Dehnen, S.; Brandmayer, M. K. *J. Am. Chem. Soc.* **2003**, *125*, 6618–6619. (d) Ruzin, E.; Dehnen, S. *Z. Anorg. Allg. Chem.* **2006**, *632*,

749−755. (e) Ruzin, E.; Zimmermann, C.; Hillebrecht, P.; Dehnen, S. *Z. Anorg. Allg. Chem.* **2007**, *633*, 820−829. (f) Lips, F.; Dehnen, S. *Inorg. Chem.* **2008**, *47*, 5561−5563. (g) Palchik, O.; Iyer, R. G.; Liao, J. H.; Kanatzidis, M. G. *Inorg. Chem.* **2003**, *42*, 5052−5054.
(9) (a) Li, J.; Chen, Z.; Emge, T. J.; Yuen, T.; Proserpio, D. M. *Inorg. Chim. Acta* **1998**, *273*, 310−315. (b) Shreeve-Keyer, J. L.; Warren, C. J.; Dhingra, S. S.; Haushalter, R. C. *Polyhedron* **1997**, *16*, 1193−1199. (c) Behrens, M.; Scherb, S.; Näther, C.; Bensch, W. *Z. Anorg. Allg. Chem.* **2003**, *629*, 1367−1373. (d) Pienack, N.; Lehmann, S.; Lühmann, H.; El-Madani, M.; Näther, C.; Bensch, W. *Z. Anorg. Allg. Chem.* **2008**, *634*, 2323−2329. (e) Liu, G. N.; Guo, G. C.; Zhang, M. J.; Guo, J. S.; H. Zeng, Y.; Huang, J. S. *Inorg. Chem.* **2011**, *50*, 9660−9669. (f) Pienack, N.; Lehmann, S.; Lühmann, H.; El-Madani, M.; Näther, C.; Bensch, W. *Z. Anorg. Allg. Chem.* **2008**, *634*, 2323−2329.
(10) (a) Chen, J. F.; Jin, Q. Y.; Pan, Y. L.; Zhang, Y.; Jia, D. X. *Chem. Commun.* **2009**, 7212−7214. (b) Liang, J. J.; Chen, J. F.; Zhao, J.; Pan, Y. L.; Zhang, Y.; Jia, D. X. *Dalton Trans.* **2011**, *40*, 2631−2637.
(11) (a) Wu, M.; Emge, T. J.; Huang, X. Y.; Li, J.; Zhang, Y. *J. Solid State Chem.* **2008**, *181*, 415−422. (b) Wu, M.; Su, W.; Jasutkar, N.; Huang, X. Y.; Li, J. *Mater. Res. Bull.* **2005**, *40*, 21−27.
(12) Manos, M. J.; Iyer, R. G.; Quarez, E.; Liao, J. H.; Kanatzidis, M. G. *Angew. Chem., Int. Ed.* **2005**, *44*, 3552−3555.
(13) (a) Brandmayer, M. K.; Clérac, R.; Weigend, F.; Dehnen, S. *Chem. Eur. J.* **2004**, *10*, 5147−5157. (b) Ruzin, E.; Fuchs, A.; Dehnen, S. *Chem. Commun.* **2006**, 4796−4698.
(14) Lin, Y.; Dehnen, S. *Inorg. Chem.* **2011**, *50*, 7913−7915.
(15) (a) Zhao, J.; Liang, J. J.; Chen, J. F.; Pan, Y. L.; Zhang, Y.; Jia, D. X. *Inorg. Chem.* **2011**, *50*, 2288−2293. (b) Jia, D. X.; Zhao, J.; Pan, Y. L.; Tang, W. W.; Wu, B.; Zhang, Y. *Inorg. Chem.* **2011**, *50*, 7195−7201. (c) Tang, C. Y.; Wang, F.; Jiang, W. Q.; Zhang, Y.; Jia, D. X. *Inorg. Chem.* **2013**, *52*, 10860−10868.
(16) Wendlandt, W. W.; Hecht, H. G. *Reflectance Spectroscopy*; Interscience: New York, 1966.
(17) *CrystalClear, Version 1.35*; Rigaku Corp., Tokyo, Japan, 2002.
(18) (a) Sheldrick, G. M. *SHELXS-97, Program for Crystal Structure Determination*; University of Göttingen, Göttingen, Germany, 1997. (b) Sheldrick, G. M. *SHELXL-97, Program for the Refinement of Crystal Structures*; University of Göttingen, Göttingen, Germany, 1997.
(19) (a) Lescouëzec, R.; Lloret, F.; Julve, M.; Vaissermann, J.; Verdaguer, M. *Inorg. Chem.* **2002**, *41*, 818−826. (b) Colacio, E.; Domínguez-Vera, J. M.; Lloret, F.; Sánchez, J. M. M.; Kivekäs, R.; Rodríguez, A.; Sillanpää, R. *Inorg. Chem.* **2003**, *42*, 4209−4214.
(20) Loose, A.; Sheldrick, W. S. *Z. Naturforsch., B* **1998**, *53b*, 349−354.
(21) Sheldrick, W. S.; Braunbeck, H.-G. *Z. Naturforsch., B* **1992**, *47b*, 151−153.

dx.doi.org/10.1021/ic501381v | *Inorg. Chem.* 2014, 53, 9267−9273